Highly conducting graphene sheets and Langmuir–Blodgett films

XIAOLIN LI[1], GUANGYU ZHANG[1], XUEDONG BAI[2], XIAOMING SUN[1], XINRAN WANG[1], ENGE WANG[2] AND HONGJIE DAI[1]*

[1]Department of Chemistry and Laboratory for Advanced Materials, Stanford University, Stanford, California 94305, USA
[2]Institute of Physics, Chinese Academy of Sciences, Beijing 100080, China
*e-mail: hdai@stanford.edu

Published online: 1 August 2008; doi:10.1038/nnano.2008.210

Graphene is an intriguing material with properties that are distinct from those of other graphitic systems[1–5]. The first samples of pristine graphene were obtained by 'peeling off'[2,6] and epitaxial growth[5,7]. Recently, the chemical reduction of graphite oxide was used to produce covalently functionalized single-layer graphene oxide[8–15]. However, chemical approaches for the large-scale production of highly conducting graphene sheets remain elusive. Here, we report that the exfoliation–reintercalation–expansion of graphite can produce high-quality single-layer graphene sheets stably suspended in organic solvents. The graphene sheets exhibit high electrical conductance at room and cryogenic temperatures. Large amounts of graphene sheets in organic solvents are made into large transparent conducting films by Langmuir–Blodgett assembly in a layer-by-layer manner. The chemically derived, high-quality graphene sheets could lead to future scalable graphene devices.

Several methods have been explored to date to obtain graphene in solution phase by means of chemical routes. Graphite oxide (GO) has been prepared by harsh oxidation using Hummer's method[16]. The as-made GO obtained in this way is electrically insulating, but chemical reduction[9,10,15] partially recovers the conductivity, albeit at values orders of magnitude below that of pristine graphene. Irreversible defects and disorder exist in the GO sheets[9,10]. The reduced GO exhibits non-metallic behaviour, with the conductance decreasing by about three orders of magnitude upon cooling to low temperatures[13], whereas pristine graphene is nearly metallic[2,17]. Recently, we obtained high quality graphene nanoribbons (GNR) by sonicating thermally exfoliated graphite in a 1,2-dichloroethane (DCE) solution of poly(m-phenylenevinylene-co-2,5-dioctoxy-p-phenylenevinylene) (PmPV)[18]. However, the yield was low and most of the ribbons had two or more layers. Despite these and other efforts[8–15,19–22], solution phase derivation of single-layer graphene with high electrical conductivity from widely available parent graphite materials has not been achieved on a large scale. The production of stable suspensions of graphene in organic solvents is also an important goal in chemical processing and other areas.

In the current work, to make high-quality graphene sheets (GS), we started by first exfoliating commercial expandable graphite (160–50 N, Grafguard) by brief (60 s) heating to 1,000 °C in forming gas. We then ground the exfoliated graphite, reintercalated it with oleum (fuming sulphuric acid with 20% free SO_3), and inserted tetrabutylammonium hydroxide (TBA, 40% solution in water) into the oleum-intercalated graphite (Fig. 1a) in *N*,*N*-dimethylformamide (DMF, see Methods). We then sonicated the TBA-inserted oleum-intercalated graphite (Fig. 1b) in a DMF solution of 1,2-distearoyl-sn-glycero-3-phosphoethanolamine-N-[methoxy(polyethyleneglycol)-5000] (DSPE-mPEG) for 60 min to form a homogeneous suspension. Centrifugation was used to remove large pieces of material from the supernatant (Fig. 1c; see also Methods). This method resulted in large amounts of GS suspended in DMF and can be transferrable to other solvents including water and organic solvents.

We used atomic force microscopy (AFM) to characterize the materials deposited on the substrates from the supernatant and observed that ~90% of the graphene sheets were single-layer GS of various shapes and sizes (Fig. 1d). For the hundreds of GS measured, we found that the average size of single-layer GS was ~250 nm (see Supplementary Information, Fig. S2a) and the average topographic height was ~1 nm (see Supplementary Information Figs. S2b and S3). Transmission electron microscopy (TEM, Fig. 1e) and electron diffraction (ED, Fig. 1f) were used to characterize the single-layer GS. The ED pattern of our GS was similar to that of peeled-off graphene[23], suggesting a well-crystallized, single-layer graphene structure.

Our starting expandable graphite was prepared by chemical intercalation of sulphuric acid and nitric acid[24]. Upon heating, they exfoliated violently due to volatile gaseous species released from the intercalant. Most of the exfoliated graphite was still in a multilayer graphene form[25]. In order to obtain single-layer GS, we used a process of reintercalation with oleum, a chemical known to strongly debundle carbon nanotubes through intercalation[26]. TBA is a molecule capable of inserting into and expanding the distance between heavily oxidized graphite layers[27]. We proposed that TBA could insert into oleum-intercalated graphite to increase the distance between adjacent graphitic layers (Fig. 1a), facilitating the separation of GS upon sonication in a surfactant solution[27]. The success of this step was made evident by showing that without this TBA treatment step, with the rest of the method being otherwise identical, the yield of single-layer GS was extremely low (see Supplementary Information, Fig. S1, for control experiments). We also found that DMF was a better solvent than water for our method. DSPE-mPEG is a surfactant capable of suspending nanotubes[28], another important factor in obtaining a homogeneous suspension of GS.

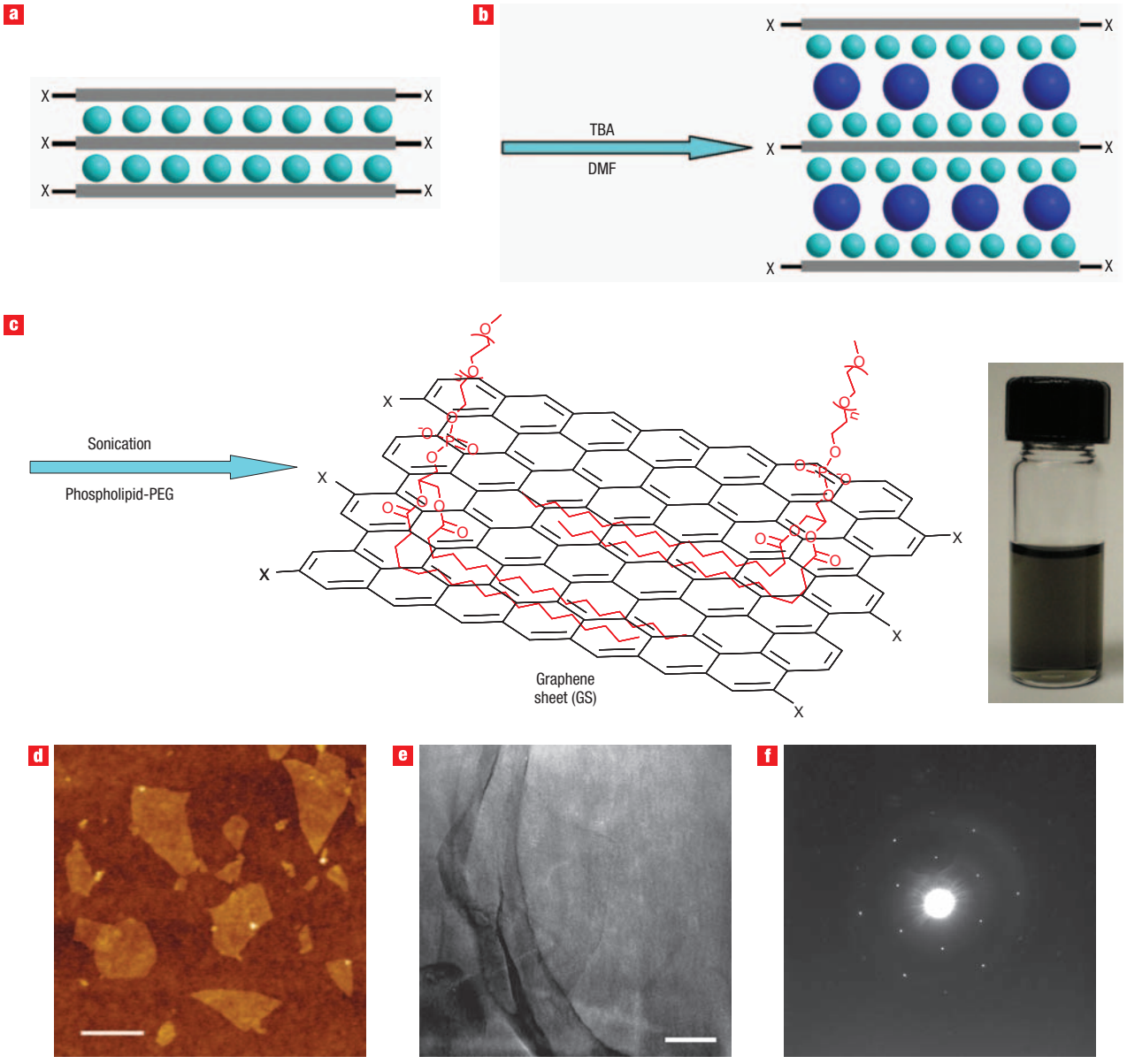

Figure 1 Chemically derived single-layer GS from the solution phase. a, Schematic of the exfoliated graphite reintercalated with sulphuric acid molecules (teal spheres) between the layers. **b**, Schematic of TBA (blue spheres) insertion into the intercalated graphite. **c**, Schematic of GS coated with DSPE-mPEG molecules and a photograph of a DSPE-mPEG/DMF solution of GS. **d**, An AFM image of a typical GS several hundred nanometres in size and with a topographic height of ~1 nm (see Supplementary Information for height details). The scale bar is 300 nm. **e**, Low- magnification TEM images of a typical GS several hundred nanometres in size. The scale bar is 100 nm. **f**, Electron diffraction (ED) pattern of an as-made GS as in **e**, showing excellent crystallization of the GS.

Our weak oleum treatment condition (soaking in oleum at room temperature for one day) is important to obtain high-quality GS without excessive chemical functionalization and thus property degradation. The conjugate graphene plane is largely free of irreversible modifications throughout the treatment steps. Room-temperature oleum treatment is much less oxidative than Hummer's method, as is clear from the infrared (IR) spectra, which show that as-made GS has significantly fewer functional groups (Fig. 2a,b) than as-made Hummer's GO (Fig. 2d,e). The IR spectrum of as-made GS (Fig. 2a) showed weaker signals for the carboxylic groups than the Hummer's GO (shaded areas in Fig. 2a,d)[29]. X-ray photoelectron spectroscopy (XPS) (Fig. 2b) of our as-made GS showed small but noticeable signals at higher binding energy corresponding to small amounts of C–O species[9,29]. These species were removed by 800 °C annealing in H_2, indicating the formation of high-quality graphene (Fig. 2b). The annealed GS exhibited the same XPS spectrum as a pristine highly oriented pyrolytic graphite (HOPG) crystal (Fig. 2b), confirming the lack of significant defects or covalent modifications of sp^2 carbon in the final GS product.

We propose the schematic structures of the intermediate and final products of our GS and Hummer's GO as shown in Fig. 2c,f. Oxidization of our intermediate, as-made GS was relatively mild, and the few covalently attached functional groups such as the carboxylic (seen in the IR spectrum, Fig. 2a) and hydroxyl groups were most likely at the edges of the as-made GS (Fig. 2c).

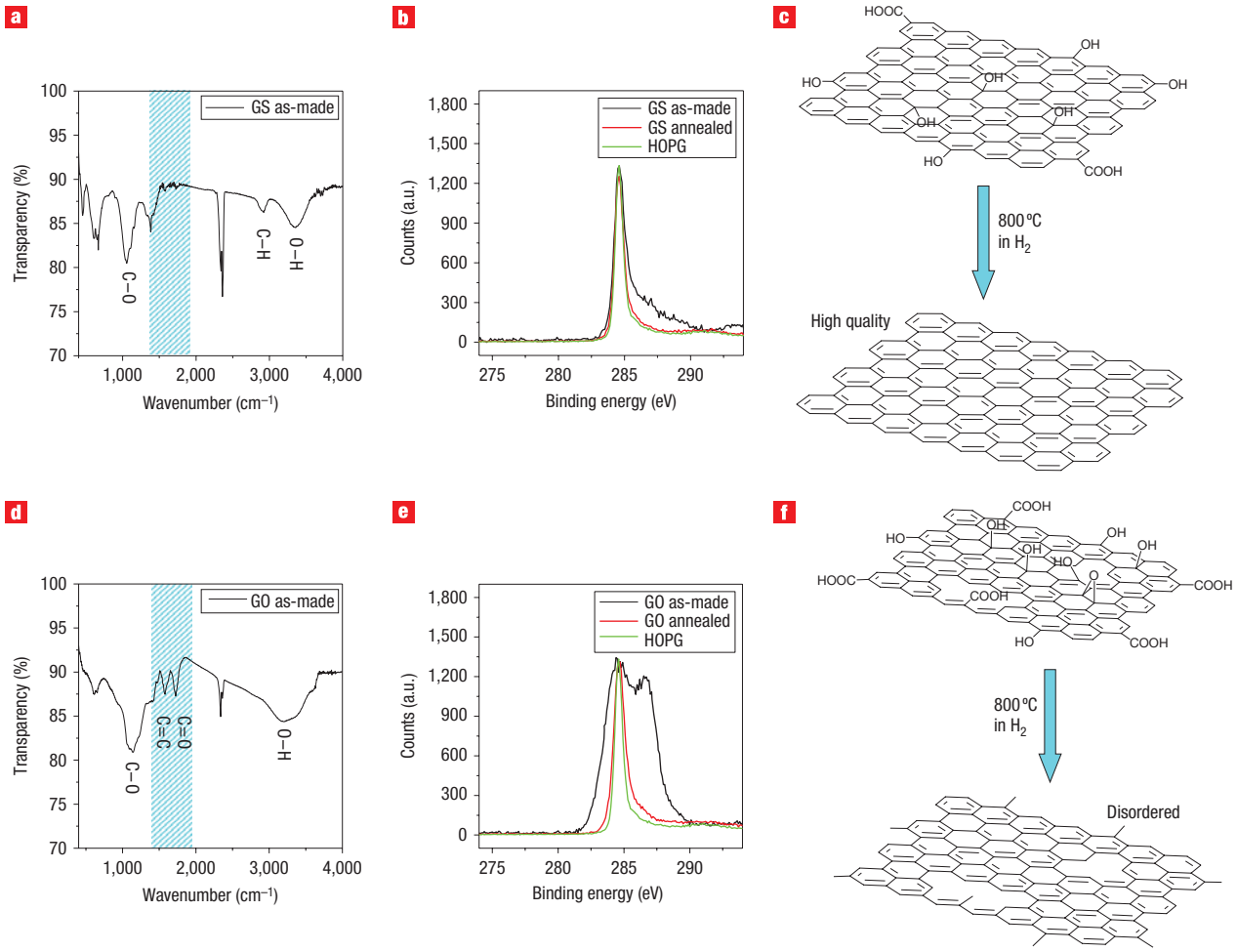

Figure 2 Comparison of GS and GO sheets. a, IR spectrum (400–4,000 cm^{-1}) of as-made GS. The shaded region from ~1,400 to 1,900 cm^{-1} includes the signal of the carboxylic groups. **b**, XPS spectra of as-made, annealed GS and a HOPG crystal. Note the similarity between the spectra of the annealed GS and HOPG. **c**, Schematic of the atomic structure of as-made (top) and annealed GS. **d**, IR spectrum (400–4,000 cm^{-1}) of as-made GO. The shaded region from ~1,400 to 1,900 cm^{-1} includes the signal of the carboxylic groups. **e**, XPS spectra of as-made, annealed GO and a HOPG crystal. **f**, Schematic of the atomic structure of as-made (top) and annealed GO.

This was supported by the fact that the electrical conductivity of our as-made GS was similar to that of 800 °C vacuum-annealed GS (Fig. 3b,c), an unlikely result if the graphene plane was heavily modified covalently. The Hummer's GO was heavily oxidized, with disrupted conjugation in the plane, missing carbon atoms in the plane[30], and abundant functional groups such as epoxide, hydroxyl, carbonyl and carboxyl at both the edges and in the plane (Fig. 2f)[9,10]. Importantly, these abundant functional groups weaken the van der Waals interactions between the layers of GO and make them hydrophilic, which is the reason for the occurrence of single-layer GO exfoliation in aqueous media to form stable suspensions without the need for an insertion agent such as TBA or the assistance of a surfactant for suspension. Thermal annealing removed some of the functional groups but was unable to completely repair the holes and other irreversible defects formed within the plane of the Hummer's GO sheets (Fig. 2f)[9,10].

We fabricated single-GS electrical devices with as-made and annealed GS and Hummer's GO. We used palladium or titanium/gold as source/drain (S/D) metal contacts (channel length $L \approx 100$ nm), a P^{++}-Si backgate and 500-nm SiO_2 for the gate dielectrics (see Methods and Supplementary Information). A typical resistance for ~100-nm-wide GS (Fig. 3a) at room temperature is 10–30 kΩ (Fig. 3b,c). The average resistance histogram (error bar is the standard deviation) for large numbers of devices showed that the room-temperature resistance of as-made GS was similar to that of annealed GS devices (for both palladium and titanium/gold contacted devices), and about 100 times lower than annealed GO (Fig. 3b). As-made GO devices without annealing were all electrically insulating. This result strongly supports the proposed atomic structures of GS and GO (Fig. 2c,f) and the assertion that our GS comprise nearly pristine graphene. Our thermally annealed GS retained high electrical conductivity, with only a slight increase in resistance at low temperatures (for both palladium and titanium/gold contacted devices), in strong contrast to annealed GO, which was insulating at low temperatures (Fig. 3c). Devices comprised of as-made GS showed reduced metallic characteristics over annealed GS devices (but were still >1,000 times more conducting than GO devices) with a larger increase in resistance at low temperatures (Fig. 3c). This suggested the as-made GS contained a small amount of disorder in the structures.

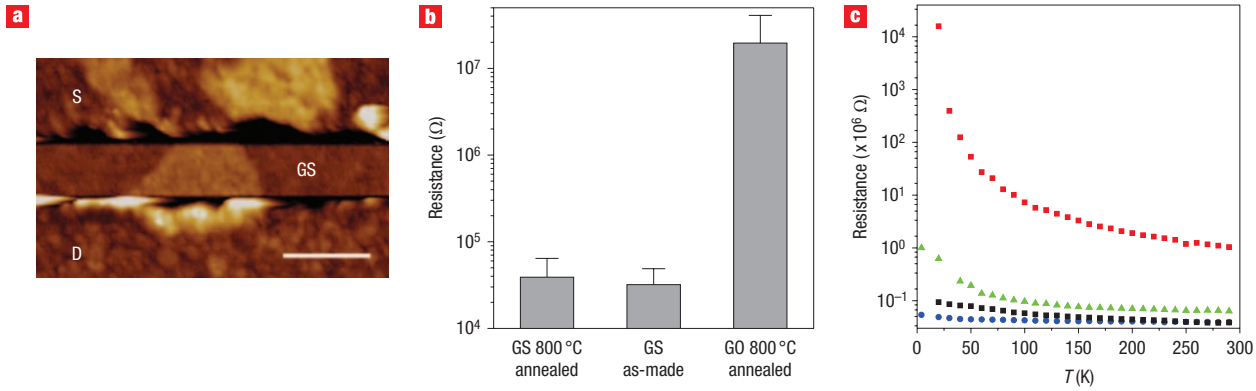

Figure 3 Electrical characterization of a single GS. a, AFM image of a typical device with a single GS (thickness ~1 nm, single layer) bridging the channel (channel length $L \approx 100$ nm GS with titanium/gold contacts and silicon backgate) between the source (S) and drain (D) electrodes. The scale bar is 200 nm. **b**, Mean resistance histograms for 10 devices each of as-made GS, annealed GS and annealed GO. The resistances of as-made GS and annealed GS were similar (within the error bars representing statistical variations between the GS devices) indicating the high quality of our as-made GS. **c**, Resistances of as-made GS (green curve), GS annealed at 800 ºC with a titanium/gold contact (black); GS annealed at 800 ºC with a palladium contact (blue), and GO annealed at 800 ºC (red). The resistance of GS, particularly the annealed GS, showed only a very small drop in conductance (similar to some of the peel-off pristine graphene samples reported in the literature) at low temperature.

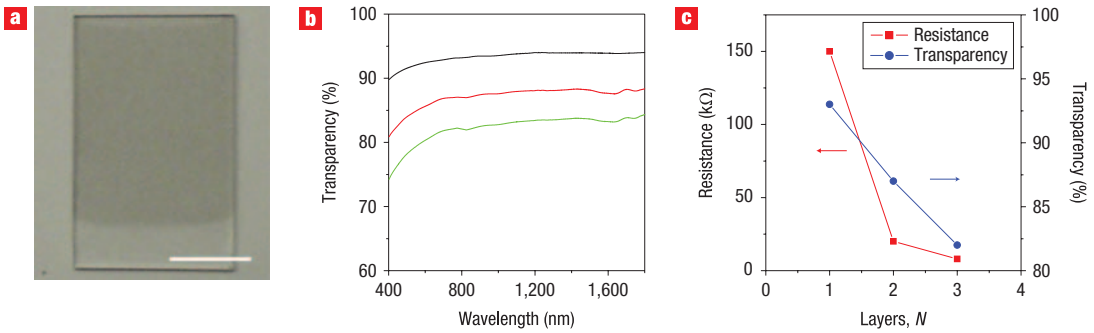

Figure 4 Large-scale Langmuir-Blodgett (LB) films of GS. a, A photograph of a two-layer GS LB film on quartz with part of it left clear. The scale bar is 10 mm. **b**, Transparency spectra of one- (black curve), two- (red curve) and three-layer (green curve) GS LB films. The transparency was defined as the transmittance at a wavelength of 1,000 nm. **c**, Resistances (red) and transparencies (blue) of one-, two- and three-layer LB films. The small percentage of bilayer and few-layer GS in our sample and GS overlapping in the LB film over the substrate contributed to the transparency loss.

To explore the utility of our high-quality GS, we transferred large quantities of GS from DMF to organic solvent DCE, with excellent stability against agglomeration. The fact that our as-made GS was stably suspended in DCE without the use of additional surfactant indicates high hydrophobicity of the graphene, consistent with a low degree of graphene oxidation and covalent functionalization. In contrast, Hummer's GO was highly hydrophilic and completely insoluble in organic solvents. The organic stability of our GS enabled Langmuir–Blodgett (LB) films to be made on various transparent substrates, including glass and quartz (see Methods and Supplementary Information) to produce transparent and conducting films. This was done by adding GS suspensions onto the water subphase, vaporizing the DCE solvent from the water surface, compressing the floating GS, and transferring the GS LB film onto a substrate by dip-coating. The GS floated on water due to the hydrophobicity within the sheet. The edges of the GS contain functional groups, giving rise to planar amphiphilic species. We were able to transfer the GS repeatedly to achieve multilayer films. The one-, two- and three-layer LB films on quartz (Fig. 4a) afforded sheet resistances of ~150, 20 and 8 kΩ at room temperature (Fig. 4c) and transparencies (defined as transmittance at a wavelength of 1,000 nm) of ~93, 88 and 83%, respectively (Fig. 4b,c). With a three-layer LB film, a sheet resistance of 8 kΩ can be achieved with a transparency greater than 80%, which compares favourably with reduced GO films[11,12]. The conductance and transparency of our films are comparable to those made of GS formed by sonication of natural graphite in DMF[31]. This is the first time that high-quality GS have been assembled by the LB technique in a layer-by-layer manner on large substrates. Note that with the same method we also succeeded in making GS using pristine graphite flakes as the starting material, and the structural, electrical and spectroscopic properties of the GS made from pristine flakes were similar to those made from expandable graphite. Thus, our large-scale synthesis of GS and the ability to process it in various solvents for assembly enables its potential use in high-performance, scalable applications such as solar cells using transparent conducting films.

METHODS

PREPARATION OF GRAPHENE SHEET SUSPENSION

Our single-layer GS preparation started by exfoliating expandable graphite (160–50 N of Grafguard) at 1,000 °C in forming gas for 60 s. Exfoliated graphite (~10 mg) was then ground with NaCl crystallites for 3 min, forming a uniform greyish mixture. Small pieces of exfoliated graphite were separated and collected by dissolving the NaCl with water and then filtration. The resulting sample was then treated with oleum at room temperature for a day. After complete removal of acid by filtration and repeated washing, the resulting sample was ultrasonicated using a cup-horn sonicator in a DMF (10 ml) solution of TBA (130 μl) for 5 min. The suspension was held at room temperature for 3 days to allow the TBA to fully insert into the graphene layers. A 5 ml suspension was then taken out and bath-sonicated with DSPE-mPEG (Laysan Bio.) (15 mg) for 1 h, forming a homogeneous suspension. After centrifuging the suspension at 24,000*g* for 3 min, we obtained a black suspension with predominantly single-layer GS retained in the supernatant.

CHARACTERIZATION OF GRAPHENE SHEETS

AFM images were taken of the GS with a Nanoscope IIIa multimode instrument. The samples were prepared by soaking a SiO_2 substrate (pretreated with a 4 mM 3-aminopropyltriethoxysilane (APTES) water solution for 20 min) in the graphene suspension for 20 min, rinsing with water and blow-drying with argon. The substrate was calcined to 350 °C and annealed at 800 °C in H_2 before AFM. The IR spectrum (400–4,000 cm^{-1}) was measured using a Nicolet IR100 FT-IR spectrometer with pure KBr as the background. After removal of the surfactant by filtration and repeated washing, the graphene sample was collected and ground with KBr. The mixture was dried and compressed into a transparent tablet for measurement. We characterized our GS using a JEOL 2010F FEG transmission electron microscope (TEM) at an accelerating voltage of 120 kV. The TEM samples were prepared by drying a droplet of the graphene suspension on a lacey carbon grid. High-resolution XPS measurement was carried out using an SSI S-Probe monochromatized XPS spectrometer, which used Al (Kα) radiation as a probe. The analysis spot size was 150 × 800 μm. Sample preparation involved removal of the surfactant by filtration and repeated washing, and depositing the materials onto a silicon substrate by repeated drop-drying. The GO sample was prepared by depositing materials onto a silicon substrate by repeated drop-drying. The HOPG sample was used for XPS measurement without any treatment.

GRAPHENE SHEET AND GRAPHITE OXIDE DEVICE FABRICATION

GS and GO were deposited onto a 500-nm $SiO_2/P^{++}Si$ substrate (pretreated with 4 mM APTES solution). After removal of the surfactant by 350 °C calcination and 800 °C H_2 annealing, we used electron-beam lithographic patterning followed by electron-beam evaporation of palladium (20 nm) or titanium (1.5 nm)/gold (20 nm) to randomly form the source and drain electrodes (channel length ~100 nm, width ~2 μm) on the substrate. The sample was then annealed in argon at 300 °C for 15 min to improve the contacts between the source and drain metal and the GS/GO in the channel region.

LANGMUIR–BLODGETT FILM FABRICATION

The DMF suspension of GS was centrifuged at 24,000*g* for 1 h to remove the surfactants. The aggregates were then resuspended in fresh DMF by a brief sonication step. This centrifugation and resuspending process was repeated three times. The GS samples were then resuspended in fresh DCE and the centrifugation and resuspending process repeated a further three times to ensure complete removal of the DSPE-mPEG. The resulting GS were suspended in DCE by a 5-min sonication step. GS LB films were made using a commercial KSV-Minimicro 2000 LB trough. Approximately 1.2 ml of GS/DCE suspension was added to a water subphase in the LB trough. A platinum plate was used to monitor the surface tension during compression of the GS on the water subphase by moving the two opposing barriers towards each other. At a target surface pressure of ~27 mN m^{-1}, GS were compressed to form a dense LB film transferrable onto a solid substrate (up to 1 × 1 $inch^2$) by slowly pulling the substrate out of the aqueous subphase. The transferred GS LB film was typically calcined at 350 °C to remove DSPE-mPEG and TBA residues before transparency and resistance measurement. After calcination of the quartz substrate with a one-layer LB film we then transferred another layer GS film onto it by repeating the LB procedure. We were able to obtain multilayer LB films by this layer-by-layer transfer method. The transparency of the GS films was measured with a Cary 6000i spectrophotometer using pure quartz as the background. The transparency was defined as the transmittance at a wavelength of 1,000 nm.

Received 31 March 2008; accepted 27 June 2008; published 1 August 2008.

References

1. Geim, A. K. & Novoselov, K. S. The rise of graphene. *Nature Mater.* **6,** 183–191 (2007).
2. Novoselov, K. S. *et al.* Electric field effect in atomically thin carbon films. *Science* **306,** 666–669 (2004).
3. Novoselov, K. S. *et al.* Two-dimensional gas of massless Dirac fermions in graphene. *Nature* **438,** 197–200 (2005).
4. Zhang, Y. B., Tan, Y. W., Stormer, H. L. & Kim, P. Experimental observation of the quantum Hall effect and Berry's phase in graphene. *Nature* **438,** 201–204 (2005).
5. Berger, C. *et al.* Electronic confinement and coherence in patterned epitaxial graphene. *Science* **312,** 1191–1196 (2006).
6. Novoselov, K. S. *et al.* Two-dimensional atomic crystals. *Proc. Natl Acad. Sci. USA* **102,** 10451–10453 (2005).
7. Berger, C. *et al.* Ultrathin epitaxial graphite: 2D electron gas properties and a route toward graphene-based nanoelectronics. *J. Phys. Chem. B* **108,** 19912–19916 (2004).
8. Dikin, D. A. *et al.* Preparation and characterization of graphene oxide paper. *Nature* **448,** 457–460 (2007).
9. Stankovich, S. *et al.* Stable aqueous dispersions of graphitic nanoplatelets via the reduction of exfoliated graphite oxide in the presence of poly(sodium 4-styrenesulfonate). *J. Mater. Chem.* **16,** 155–158 (2006).
10. Stankovich, S. *et al.* Synthesis of graphene-based nanosheets via chemical reduction of exfoliated graphite oxide. *Carbon* **45,** 1558–1565 (2007).
11. Gilje, S., Han, S., Wang, M. S., Wang, K. L. & Kaner, R. B. A chemical route to graphene for device applications. *Nano Lett.* **7,** 3394–3398 (2007).
12. Li, D., Muller, M. B., Gilje, S., Kaner, R. B. & Wallace, G. G. Processable aqueous dispersions of graphene nanosheets. *Nature Nanotech.* **3,** 101–105 (2008).
13. Gomez-Navarro, C. *et al.* Electronic transport properties of individual chemically reduced graphene oxide sheets. *Nano Lett.* **7,** 3499–3503 (2007).
14. Wang, X., Zhi, L. J. & Mullen, K. Transparent, conductive graphene electrodes for dye-sensitized solar cells. *Nano Lett.* **8,** 323–327 (2008).
15. Bourlinos, A. B. *et al.* Graphite oxide: chemical reduction to graphite and surface modification with primary aliphatic amines and amino acides. *Langmuir* **19,** 6050–6055 (2003).
16. Hummers, W. S. & Offeman, R. E. Preparation of graphite oxide. *J. Am. Chem. Soc.* **80,** 1339 (1958).
17. Tan, Y. W., Zhang, Y. B., Stormer, H. L. & Kim, P. Temperature dependent electron transport in graphene. *Eur. Phys. J.* **148,** 15–18 (2007).
18. Li, X. L., Wang, X. R., Zhang, L., Lee, S. W. & Dai, H. J. Chemically derived, ultrasmooth graphene nanoribbon semiconductors. *Science* **319,** 1229–1232 (2008).
19. Stankovich, S. *et al.* Graphene-based composite materials. *Nature* **442,** 282–286 (2006).
20. Schniepp, H. C. *et al.* Functionalized single graphene sheets derived from splitting graphite oxide. *J. Phys. Chem. B* **110,** 8535–8539 (2006).
21. Yu, A. P., Ramesh, P., Itkis, M. E., Bekyarova, E. & Haddon, R. C. Graphite nanoplatelet–epoxy composite thermal interface materials. *J. Phys. Chem. C* **111,** 7565–7569 (2007).
22. Niyogi, S. *et al.* Solution properties of graphite and graphene. *J. Am. Chem. Soc.* **128,** 7720–7721 (2006).
23. Meyer, J. C. *et al.* The structure of suspended graphene sheets. *Nature* **446,** 60–63 (2007).
24. Greinke, R. A. *et al.* Expandable graphite and method. US patent 6416815 B2 (2002).
25. Han, J. H., Cho, K. W., Lee, K.-H. & Kim, H. Porous graphite matrix for chemical heat pumps. *Carbon* **36,** 1801–1810 (1998).
26. Ericson, L. M. *et al.* Macroscopic, neat, single-walled carbon nanotube fibres. *Science* **305,** 1447–1450 (2004).
27. Liu, Z. H., Wang, Z. M., Yang, X. J. & Ooi, K. Intercalation of organic ammonium ions into layered graphite oxide. *Langmuir* **18,** 4926–4932 (2002).
28. Kam, N. W. S., O'Connell, M., Wisdom, J. A. & Dai, H. J. Carbon nanotubes as multifunctional biological transporters and near-infrared agents for selective cancer cell destruction. *Proc. Natl Acad. Sci. USA* **102,** 11600–11605 (2005).
29. Hontoria-Lucas, C., Lopez-Peinado, A. J., Lopez-Gonzalez, J. de D., Rojas-Cervantes, M. L. & Martin-Aranda, R. M. Study of oxygen-containing groups in a series of graphite oxides: physical and chemical characterization. *Carbon* **33,** 1585–1592 (1995).
30. Kuznetsova, A. *et al.* Enhancement of adsorption inside of single-walled nanotubes: opening the entry ports. *Chem. Phys. Lett.* **321,** 292–296 (2000).
31. Blake, P. *et al.* Graphene-based liquid crystal device. *Nano Lett.* **8,** 1704–1708 (2008).

Supplementary Information accompanies this paper at www.nature.com/naturenanotechnology.

Acknowledgements

We thank Graftech for providing expandable graphite samples. This work was supported in part by Intel, the Microelectronics Advanced Research Corporation Materials, Structures and Devices (MARCO MSD) Focus Centre and the Office of Naval Research.

Author contributions

H.D. and X.L. conceived and designed the experiments. X.L. and G.Z. performed the experiments and analysed the data. H.D. and X.L. co-wrote the manuscript. All authors discussed the results and commented on the manuscript.

Author information

Reprints and permission information is available online at http://npg.nature.com/reprintsandpermissions/. Correspondence and requests for materials should be addressed to H.D.